This article has been accepted for publication in IEEE Transactions on Mobile Computing. This is the author's version which has not been fully edited and content may change prior to final publication. Citation information: DOI 10.1109/TMC.2022.3181038

Age of Information Optimization in Multi-Channel based Multi-hop Wireless Networks

Jiadong Lou, *Student Member, IEEE,* Xu Yuan, *Senior Member, IEEE,* Purushottam Sigdel, *Member, IEEE,* Xiaoqi Qin, *Member, IEEE,* Sastry Kompella, *Senior Member, IEEE,* and Nian-Feng Tzeng, *Life Fellow, IEEE*

Abstract—The proliferation of IoT devices, with various capabilities in sensing, monitoring, and controlling, has prompted diverse emerging applications, highly relying on effective delivery of sensitive information gathered at edge devices to remote controllers for timely responses. To effectively deliver such information/status updates, this paper undertakes a holistic study of AoI in multi-hop networks by considering the relevant and realistic factors, aiming for optimizing information freshness by rapidly shipping sensitive updates captured at a source to its destination. In particular, we consider the multi-channel with OFDM (orthogonal frequency-division multiplexing) spectrum access in multi-hop networks and develop a rigorous mathematical model to optimize AoI at destination nodes. Real-world factors, including orthogonal channel access, wireless interference, and queuing model, are taken into account for the very first time to explore their impacts on the AoI. To this end, we propose two effective algorithms where the first one approximates the optimal solution as closely as we desire while the second one has polynomial time complexity, with a guaranteed performance gap to the optimal solution. The developed model and algorithms enable in-depth studies on AoI optimization problems in OFDM-based multi-hop wireless networks. Numerical results demonstrate that our solutions enjoy better AoI performance and that AoI is affected markedly by those realistic factors taken into our consideration.

Index Terms—Age of Information, Multi-hop wireless networks, OFDM, Queuing models, Wireless interference.

1 Introduction

The prosperity of Cyber-Physical Systems (CPS) and Internet of Things (IoT) has prompted diverse emerging applications in smart cities, intelligent transportation systems, automatic industrial plants, weather forecasting, among others. Deployments of such emerging applications often involve many edge devices (e.g., sensors) scattered across the covered areas, and their backbones lie in punctual delivery of sensitive information/updates gathered by these devices for the receivers of interest, where the multi-hop relays are necessary to extend the network coverage to a wide area. For instance, in a weather forecasting system, numerous wireless devices can be deployed across a broad area that is far away from the emergency control center. Due to the proliferation of these edge devices with various capabilities in sensing, monitoring, and controlling, in support of those applications, we have witnessed mounting challenges for data gathering and delivery to remote controllers for timely responses, especially when the devices involved are diverse and the device count rises.

To measure the timely information updates, a suitable performance metric that reflects information updating timeliness (i.e., freshness) has been introduced [1], [2] and exploited lately, known as *Age of Information* (AoI). Defined as the time elapsed since the generation time of the most recently received packet at a destination node, AoI is utterly a proper metric of choice to quantify information freshness. For instance, at time t, the freshest update delivered at the destination node was generated at $G(t)$, the AoI is calculated as $t - G(t)$. Such a new metric is starkly different from the conventional metrics of overall throughput and packet delay [2], which characterize the effectiveness of a data collection and transfer system but fail to capture the time-critical information updates at an individual receiver. From this point of view, AoI is substantially distinct from delay, as its variation characterizes dynamism in information updating. The previous works [1], [2], [3] also have demonstrated that optimizing AoI is fundamentally different from minimizing delay.

Up till now, AoI has been explored mostly in very simple network settings, i.e., single-hop networks [1], [2], [3], [4], [5], [6], [7], [8], [9], [10], [11], [12], [13], [14], [15], [16], [17], [18], [19], [20]. Limited pursuit in multi-hop networks deals merely with either the special network topology [21], [22], [23], [24], [25] or abstracted network settings [26], [27], [28]. The problem of how to minimize AoI in a multi-hop network remains open, especially when taking into account such realistic physical world factors as channel access techniques, wireless interference, link scheduling, among others. These realistic factors are of critical importance in transforming AoI from a concept to the real-world applications. To date, there are no prior results on AoI optimization for multi-hop networks with realistic factors taken into consideration.

This paper aims to advance the theoretical foundation of

- *Manuscript received August 15, 2021; revised February 6, 2022 and May 16, 2022; accepted May 25, 2022. Corresponding author: Dr. Xu Yuan.*
- *J. Lou, X. Yuan, P. Sigdel, and N-F. Tzeng are with the School of Computing and Informatics, University of Louisiana at Lafayette, LA, U.S. E-mail: {jiadong.lou1, xu.yuan, pxs9444, tzeng}@louisiana.edu.*
- *X. Qin is with Beijing University of Posts and Telecommunications, Beijing, China. E-mail: xiaoqiqin@bupt.edu.cn.*
- *S. Kompella is with U.S. Naval Research Laboratory, Washington.DC, U.S. E-mail: sastry.kompella@nrl.navy.mil.*

AoI in multi-hop wireless systems. It addresses the multi-hop wireless networks with the widely adopted channel access modulation, i.e., orthogonal frequency-division multiplexing (OFDM), for the first time, while taking into account relevant realistic factors so as to capture their impacts on AoI at destination nodes. In OFDM-based multi-hop networks, the channel allocation, interference, and queuing model are key factors to determine their AoI outcomes. By modeling both the arrival and the service processes at each node, we develop a mathematical model to capture the relationships of these realistic factors and AoI. The mathematical formula of AoI derived theoretically allows us to address AoI minimization in OFDM-based multi-hop networks.

As our developed optimization problem is in the form of mixed integer non-linear programming (MINLP), we propose two approximate algorithms to solve it efficiently. In the first algorithm, we employ the piece-wise linearization technique to transform the non-linear AoI formula into a set of linear constraints, enabling us to use the commercial solver to tackle it. By pre-setting a small error bound, this algorithm can find a solution very close to the optimal one. However, the linearized problem is still in the form of mixed integer linear programming (MILP), which has exponential time complexity. The commercial solvers can solve it efficiently for small-sized networks only but not for moderate or large-sized networks. We then derive the second algorithm considering the interference relationships among links, able to solve our developed model in a polynomial time. The solution gap between our algorithm and the optimal one is theoretically derived and proved, signifying the efficiency and effectiveness of our design. We have conducted simulation studies to quantify AoI performance in OFDM-based multi-hop wireless networks. The numerical results show the relationships of AoI with (1) channel resources, (2) wireless interference, and (3) packet generation rates in multi-hop networks to demonstrate the advantages of our proposed model and algorithms.

The remainder of this paper is organized as follows. Section 2 illustrates our network model. In Section 3, we develop the mathematical model and deal with the AoI minimization problem in OFDM-based multi-hop networks. In Section 4, we devise two approximate algorithms for the AoI optimization problem. In Section 5, we present the numerical AoI performance results, which exhibit the impacts of physical factors on AoI. In Section 6 and Section 7, we outline related work and discussion, respectively. Section 8 concludes the paper.

2 Network Model

In this paper, we consider a multi-hop wireless network comprising a set of nodes $\mathcal{N}$ and a number of sessions $\mathcal{L}$ as shown in Figure 2. Suppose each session has a predefined route traversing multiple nodes from a source to its destination node.

We denote s_l and d_l as the source and destination nodes of a session $l \in \mathcal{L}$, respectively, with P_l indicating its traversal path. Suppose this network has time-sensitive applications, calling for stringent requirements on information transfer freshness. To capture updating information so as to fulfill such time-sensitive application needs, we adopt *Age of Information* (AoI) as the main performance metric.

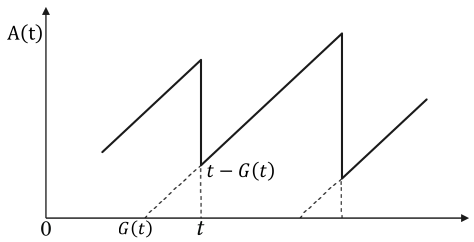

Fig. 1. AoI variation at a node i in session l.

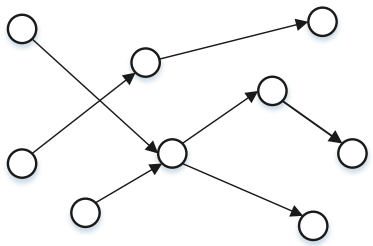

Fig. 2. An example of a multi-hop wireless network.

To model AoI at a time t, we denote $G_i^l(t)$ as the generation time of the latest arrived packet at an intermediate node i from source node s_l on path P_l. Thus, AoI for packets reaching node i at time t, denoted by $a_i^l(t)$, can be mathematically expressed as:

$$a_i^l(t) = t - G_i^l(t). \tag{1}$$

Figure 1 illustrates the variation of AoI at node i. Assume the kth packet is generated at time $t(k)$ from the source node and delivered to node i at time $\hat{t}_i(k)$. AoI increases linearly (after receiving the prior $(k-1)$th packet) until the kth packet arrival; AoI is then reduced to $\hat{t}(k) - t(k)$. After that, AoI continues to rise linearly with time t, i.e., $a_i^l(t) = t - t(k)$, until this node receives the next packet.

From Figure 1, the total aggregated AoI over a time range $(0, T)$ at node i (denoted as ΔA_i^l) can be calculated by using the graphical approach, i.e., the area under the sawtooth curve within the time range, expressed by:

$$\Delta A_i^l = \int_0^T a_i^l(t)\, dt\ . \tag{2}$$

Then, we denote the following time averaged AoI at a node i (denoted as A_i^l), i.e.,

$$A_i^l = \frac{\Delta A_i^l}{T} = \frac{1}{T}\int_0^T a_i^l(t)\, dt\ . \tag{3}$$

In this paper, we aim to explore AoI in multi-hop wireless networks under widely adopted OFDM channel access modulation, starting with developing a tactical model for AoI optimization in such wireless networks. There are a number of challenges arising for exploring AoI in multi-hop networks, including but are not limited to

- In multi-hop settings, the packet arrival procedures among intermediate nodes correlate with each other. To model AoI at a destination node, it is necessary to capture the packet arrival process at each

intermediate node. As we can only have the packet arrival process at a source node, how to model such arrival process at each intermediate node and its relationships with the arrival process at source node is a challenging problem.

- The channel allocation is critical in OFDM-based multi-hop wireless networks. There are two main purposes for channel allocation in multi-hop networks. First, scheduling the transmission of each link to ensure a packet is transported from its source to its destination. Second, the number of channels allocated to each link determines its service capability. As the significant difference of AoI and the traditional performance metrics, i.e., throughput and delay, the existing channel allocations strategy may not work here anymore. This poses new challenge to develop novel channel allocation strategy to make all links have the suitable service rates that minimize AoIs at destination nodes.
- The interference is an annoying problem in wireless networks, especially in multi-hop settings to become even much more pronounced. A set of interference constraints has to be accounted for, including half-duplex, unicast, and channels reuse, so as to ensure that all packets can be transported to destination nodes successfully. It is obviously non-trivial to capture all potential interference relationships and establish a suitable model under which all nodes can transmit and receive packets without interference in multi-hop networks.

3 Mathematical Modeling and Problem Formulation

Suppose B orthogonal channels with equal bandwidth are available in total and they are scheduled (i.e., activated) for packet transmission over links with no interference present among activated links. The route from a session's source node to its destination node is known apriori, found by a certain standard routing protocol (e.g., AODV [29] or DSR [30]). Multiple sessions may intersect at some nodes but no multiple sessions share the same link. We denote $\mathcal{R}_i$ as the set of nodes that receive packets from node i (i.e., i's successors) and denote $\mathcal{J}_i$ as the set of nodes that transmit packets to i (i.e., i's predecessors). The set of nodes located within the interference range of node i is denoted by $\mathcal{I}_i$. Table 1 lists notations employed in this paper.

To model link scheduling, we use a binary variable $n_{ij}[b]$ to indicate whether a link from node i to node j (i.e., (i,j)) is activated or not for transmitting packets in a given channel b, i.e., $n_{ij}[b]=1$, if the link (i,j) is activated in channel b; $n_{ij}[b]=0$, otherwise. We have:

$$n_{ij}[b]=\begin{cases}1, & \text{if the link } (i,j) \text{ is activated in channel } b\ ,\\ 0, & \text{otherwise.}\end{cases}$$

where $i,j\in\mathcal{N}, 1\le b\le B$, and $j\in\mathcal{R}_i$.

We assume that each session is unicast. That is, a node i can transmit to, or receive from, only one node over a channel b. Thus, we have:

$$\sum_{j\in\mathcal{R}_i} n_{ij}[b]\le 1\ , \tag{4}$$

$$\sum_{j\in\mathcal{J}_i} n_{ji}[b]\le 1\ . \tag{5}$$

To account for half-duplex at each node i, we have:

$$n_{ij}[b]+n_{zi}[b]\le 1, (i\in\mathcal{N}, j\in\mathcal{R}_i, z\in\mathcal{J}_i, 1\le b\le B). \tag{6}$$

These constraints can be replaced by the following equivalents:

$$\sum_{j\in\mathcal{R}_i} n_{ij}[b]+\sum_{z\in\mathcal{J}_i} n_{zi}[b]\le 1, (i\in\mathcal{N}, 1\le b\le B). \tag{7}$$

To avoid interference among links, we assume that if a node $j\in\mathcal{N}$ is receiving data over a channel b, it never gets interfered by another (unintended) transmitting node $p\in\mathcal{I}_j$ in the same channel. Hence, we have the following constraint:

$$n_{ij}[b]+n_{ph}[b]\le 1, \tag{8}$$

where $j\in\mathcal{N}, i\in\mathcal{J}_j, p\in\mathcal{I}_j, h\in\mathcal{R}_p, j\ne h$, and $1\le b\le B$.

3.1 Queuing Model

Let $M_{ij}^l(k)$, $W_{ij}^l(k)$, and $X_{ij}^l(k)$ denote the system time, the waiting time, and the service time, respectively, for the kth packet transmitted from a node i to its successor node j on a path P_l. Here, the waiting time $W_{ij}^l(k)$ is considered as the time interval between the kth packet reaching node i and starting to be transmitted over link (i,j). In other words, it is the time a packet stays in the queue. The service time $X_{ij}^l(k)$ is the time that link (i,j) spends in delivering the kth packet. It is the time duration of a packet from its transmission start to its transmission end over link (i,j). The system time refers to the time interval between a packet reaching the queue at a node and it finishing transmission to its successor, thereby calculated as the sum of packet's waiting time in the queue and its service time, i.e.,

$$M_{ij}^l(k)=W_{ij}^l(k)+X_{ij}^l(k). \tag{9}$$

We assume the kth packet arrives at nodes i and j at time $\hat{t}_i(k)$ and $\hat{t}_j(k)$, respectively. The propagation delay, being negligible, is not considered here, with a packet assumed for instant transfer to the next node if there are available channels on the outgoing link, so the system time $M_{ij}^l(k)$ can be calculated as

$$M_{ij}^l(k)=\hat{t}_j(k)-\hat{t}_i(k). \tag{10}$$

With $I_i^l(k)$ denoting the time interval of two consecutive packets, i.e., $(k-1)$th and kth ones, arriving at node $i, i\ne s_l$ along path P_l, we have:

$$I_i^l(k)=\hat{t}_i(k)-\hat{t}_i(k-1). \tag{11}$$

Specifically, at the source node s_l, $I_{s_l}^l(k)$ represents the time interval between the generation times of the $(k-1)$th and the kth packets, i.e.,

$$I_{s_l}^l(k)=t(k)-t(k-1). \tag{12}$$

Suppose packets at all nodes follow *First Come First Served* (FCFS) scheduling, while at each source node, the packet is generated and serviced with an $M/M/1$ queuing system. For simplicity, we assume that packets arrive at (i.e., packet generation) all source nodes following the Poisson process with the rate of λ, and that packets' service times

TABLE 1
Notations employed in this paper

$\mathcal{N}$	The set of nodes in the multi-hop network.
$\mathcal{L}$	The set of sessions in the multi-hop network.
B	The number of orthogonal channels.
D	The number of links in the multi-hop network.
s_l	The source node of a session $l \in \mathcal{L}$.
d_l	The destination node of a session $l \in \mathcal{L}$.
P_l	The traversal path of session $l \in \mathcal{L}$.
$\mathcal{P}_l$	The set of traversed nodes along a path P_l.
$G_i^l(t)$	The generation time of the latest arrived packet at a node i from source node s_l at time t.
$a_i^l(t)$	AoI for packets from the source node s_l reaching a node i at time t.
A_i^l	The time averaged AoI at a node i from source s_l.
A^{ave}	The total time averaged AoI among all sessions.
$\mathcal{R}_i$	The set of nodes that receive packets from node i.
$\mathcal{J}_i$	The set of nodes that transmit packets to node i.
$\mathcal{I}_i$	The set of nodes located within the interference range of node i.
$n_{ij}[b]$	$= 1$ if the link (i,j) is activated in a channel b; $= 0$, otherwise.
$M_{ij}^l(k)$	The system time for the kth packet transmitted from a node i to its successor node j in a path P_l.
$W_{ij}^l(k)$	The waiting time for the kth packet transmitted from a node i to its successor node j in a path P_l.
$X_{ij}^l(k)$	The service time for the kth packet transmitted from a node i to its successor node j in a path P_l.
$I_i^l(k)$	Time interval of two consecutive packets ($(k-1)$th and kth) ones, arriving at node $i, i \neq s_l$ along path P_l.
λ	The packet generation rate at source nodes.
μ_{ij}	Total service rate of a link (i,j) over all its available channels.
f_{ij}	Activation frequency of a link (i,j) on all channels.

at all nodes follow the i.i.d exponential distribution with the rate of μ at each node in every channel. If $E[\cdot]$ denotes the average value, we have $E[I_{s_l}^l] = 1/\lambda$. According to the $M/M/1$ property at source nodes, we have the following lemma.

Lemma 1. *At each node along path P_l, the packet arrival process has the same distribution as that of the packet generation process at its source node s_l, i.e.,*

$$E[I_i^l] = E[I_{s_l}^l] = 1/\lambda, \forall i \in \mathcal{P}_l, i \neq s_l, \tag{13}$$

where $\mathcal{P}_l$ represents the set of traversed nodes on path P_l.

Proof. Burke's theorem [31] is employed to prove this lemma. It asserts that, for the $M/M/1$ queue in the steady state, if the arrival is a Poisson process with a rate of λ, the departure is also a Poisson process with the same rate. Since each source node s_l is an FCFS $M/M/1$ queuing system, the departure process at the source node will follow the Poisson process with the rate of λ, which is the same as the source's arrival rate (i.e., generation rate). As packets can be immediately transmitted to the next node if there are available channels on the outgoing links, the arrival process of a packet at the second node along $\mathcal{P}_l$ must be the same as the departure process of its predecessor (i.e., the upstream source node). Multiple sessions may intersect at a certain node, at which the departure process of packets that belong to source s_l must keep the same as its packet arrival process based on Burke's theorem. Thus, at each node on its path P_l, the arrival of packets which belong to s_l will follow the Poisson process with the rate of λ. □

Since the packet arrival process follows the Poisson process and the service process is assumed to be governed by the i.i.d exponential distribution at each node, the packet transmission process can be modeled as an FCFS $M/M/1$ queue.

3.2 Link Activation Constraints

We let variable f_{ij} indicate the activation frequency of a link (i,j) among all channels, i.e.,

$$f_{ij} = \sum_{b=1}^{B} n_{ij}[b], \qquad (j \in \mathcal{R}_i). \tag{14}$$

That is, f_{ij} represents the number of channels that a link (i,j) can activate among B channels. Note here, if $f_{ij} = 0$, the link (i,j) cannot be activated in any channel. There will be no packet transmitting successfully in the associated session. In this case, the AoI will be considered as infinity, which is not our expectation. Here, we aim to have each link activated at least once, i.e.,

$$f_{ij} \geq 1, \qquad (i \in \mathcal{N}, j \in \mathcal{R}_i). \tag{15}$$

Denote the total service rate of a link (i,j) over all its available channels as μ_{ij}, which can be modeled by the link activation frequency and the service rate on each channel, i.e.,

$$\mu_{ij} = \mu f_{ij}. \tag{16}$$

Notably, in an FCFS $M/M/1$ queuing model, if the packet arrival rate is no less than the service rate at a node, the number of packets in the queue becomes infinite when the transmission process reaches stability. To avoid this undesirable situation, at each node on path P_l, we let the total service rate be greater than the arrival rate, yielding

$$\mu_{ij} = \mu f_{ij} > \lambda, \qquad (i \in \mathcal{N}, j \in \mathcal{R}_i). \tag{17}$$

3.3 AoI Formula

We start with deriving the AoI relationship of any two neighboring nodes, e.g., node i and its successor j along path P_l. This relationship later helps us to derive AoI at a destination node from its source. Let A_i^l and A_j^l denote the time averaged AoI at nodes i and j, respectively. According to the property of AoI, we have the following theorem.

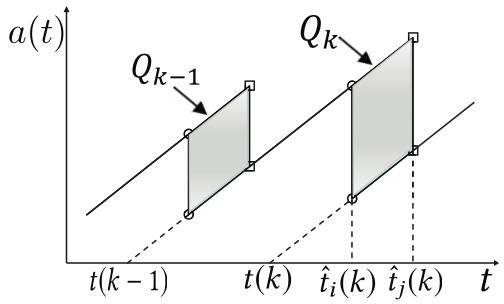

Fig. 3. AoI variations at two consecutive nodes on a path.

Theorem 1. *Time averaged AoI at a node j and its predecessor i along path P_l within the time span of $(0, T)$ satisfies the following relationship:*

$$A_j^l = A_i^l + \lambda E[I_{s_l}^l M_{ij}^l]. \tag{18}$$

Proof. In Figure 3, assume the kth packet is generated by a source node s_l at $t(k)$ and is received by nodes i and j at $\hat{t}_i(k)$ and $\hat{t}_j(k)$, respectively. Suppose the line segments with pairs of circular and square symbols represent the AoIs at nodes i and j, respectively, and each aggregated AoI is the area under its sawtooth curve. The difference of the aggregated AoIs between nodes i and j can be calculated as a sum of shadow parallelogram parts in Figure 3. Therefore, the relationship of aggregated AoIs at node j and node i can be calculated by

$$\Delta A_j^l = \Delta A_i^l + \sum_{k=1}^{K} Q_k, \tag{19}$$

where Q_k is the area of the kth parallelogram (indicated as the shadow area in Figure 3) and K is the total number of packets that are delivered within the time span $(0, T)$. Here, the area Q_k can be calculated by the product of $t(k)-t(k-1)$ and $\hat{t}_j(k) - \hat{t}_i(k)$, which are equal to $I_{s_l}^l(k)$ and $M_{ij}^l(k)$, respectively. Therefore, we have:

$$Q_k = I_{s_l}^l(k) M_{ij}^l(k). \tag{20}$$

As a result, ΔA_j^l can be rewritten as

$$\Delta A_j^l = \Delta A_i^l + \sum_{k=1}^{K} I_{s_l}^l(k) M_{ij}^l(k). \tag{21}$$

Within the time span of $(0, T)$, the time averaged AoI is

$$\begin{aligned} A_j^l &= \frac{\Delta A_j^l}{T} = A_i^l + \frac{\sum_{k=1}^{K} I_{s_l}^l(k) M_{ij}^l(k)}{T} \\ &= A_i^l + \frac{K}{T}\frac{1}{K}\sum_{k=1}^{K} I_{s_l}^l(k) M_{ij}^l(k) \\ &= A_i^l + \frac{K}{T} E[I_{s_l}^l M_{ij}^l]. \end{aligned} \tag{22}$$

Based on Lemma 1, the packet arrival rate at each node is λ. As node j has received a total of K packets within $(0, T)$ and no packet is dropped, we have:

$$\lambda = \frac{K}{T}. \tag{23}$$

As a result, the relationship of time averaged AoI of two consecutive nodes can be expressed by

$$A_j^l = A_i^l + \lambda E[I_{s_l}^l M_{ij}^l]. \tag{24}$$

□

As stated in Theorem 1, AoI at the destination node can be derived by recursive calculation from the source node. Thus, we obtain the following theorem for the time average AoI at the destination node d_l.

Theorem 2. *Time averaged AoI at destination node d_l on path P_l can be formulated as follows:*

$$A_{d_l}^l = \frac{1}{\lambda} + \sum_{i \in \mathcal{P}_l, i \neq d_l} \left(\frac{1}{\mu f_{ij}} + \frac{\lambda^2}{(\mu f_{ij})^2(\mu f_{ij} - \lambda)}\right), \tag{25}$$

where node j is node i's successor.

This theorem is derived from Theorem 1, by traversing all links along each session l until reaching its destination node d_l. The detailed proof is deferred to Appendix A.1.

From Theorem 2, we have the total time averaged AoI among all sessions, denoted by A^{ave}, as follows:

$$\begin{aligned} A^{ave} &= \sum_{l \in \mathcal{L}} \left(\frac{1}{\lambda} + \sum_{i \in \mathcal{P}_l}^{i \neq d_l} \left(\frac{1}{\mu f_{ij}} + \frac{\lambda^2}{(\mu f_{ij})^2(\mu f_{ij} - \lambda)}\right)\right) \\ &= \frac{|\mathcal{L}|}{\lambda} + \sum_{i \in \mathcal{N}} \sum_{j \in \mathcal{R}_i} \left(\frac{1}{\mu f_{ij}} + \frac{\lambda^2}{(\mu f_{ij})^2(\mu f_{ij} - \lambda)}\right). \end{aligned} \tag{26}$$

3.4 Problem Formulation

With the developed model, we are interested in minimizing the total time averaged AoI at all destination nodes, as formulated next.

$$\begin{aligned} \text{OPT-O} \quad & \min A^{ave} \\ & s.t. \text{ The total time averaged AoI function: } (26); \\ & \quad \text{Interference constraints: } (7),\ (8); \\ & \quad \text{Links activation frequency: } (14); \\ & \quad \text{Queuing model constraint: } (17). \end{aligned}$$

where $\mathcal{L}$, μ, and λ are constant. f_{ij} and $n_{ij}[b]$ are integer and binary variables, respectively, which are to be solved for optimizing the total time averaged AoI A^{ave}. Due to non-linear terms in the objective function, the optimization problem is in the form of *mixed-integer non-linear programming* (MINLP), which is NP-hard in general. Two approximate algorithms are then provided next to solve this problem.

4 Algorithm Design

In this section, we provide two approximate algorithms to solve the optimization problem of OPT-O. In the first algorithm, we aim to design a solution that can approach the optimal one as closely as possible by pre-setting the required approximate error bound. We make use of the piece-wise linearization technique to linearize the objective function and then solve it by using the commercial solver. This algorithm approaches closer to the optimal solution by setting a smaller approximation error bound, but it has high computation complexity, making it unsuitable for moderate

or large-sized networks. In the second algorithm, we design a polynomial time solution to solve OPT-O and theoretically prove the gap between our algorithm's solution and the optimal one.

4.1 Linearized Approximate Algorithm

Considering the commercial solver, such as CPLEX, can help to solve the linear programming problem, here, the main idea of this linear approximate algorithm is to replace the nonlinear function in the problem by linear segments, which is called piece-wise linearization. Moreover, the proposed algorithm constructs these linear segments within any given difference compared to the original function, in other words, the performance bound of the approximate solution is controllable. However, the closer to optimal, the more segments are needed, resulting in longer processing times in CPLEX.

In OPT-O, the non-linear part is in the objective function. So, we define a new function as

$$h(x) = \frac{1}{\mu x} + \frac{\lambda^2}{(\mu x)^2(\mu x - \lambda)} ,$$

and replace the objective function with

$$A^{ave} = \frac{|\mathcal{L}|}{\lambda} + \sum_{i\in\mathcal{N}} \sum_{j\in\mathcal{R}_i} h(f_{ij}). \tag{27}$$

Since f_{ij} is in the range of $[\frac{\lambda}{\mu}, B]$ (from Constraints (14) and (17)), we have

$$\frac{\partial h(x)}{\partial x^2} = \frac{2}{\mu x^3} - \frac{2\lambda^2\left(3\lambda^3 - 11\lambda^2\mu x + 14\lambda\mu^2x^2 - 6\mu^3x^3\right)}{\mu^2x^4\left(\mu x - \lambda\right)^4} > 0$$

Thus, $h(f_{ij})$ is a convex function. This allows us to employ the piece-wise linearization technique to approximate the curve of $h(f_{ij})$. Our goal here is to replace each $h(f_{ij})$ with a minimum set of linear segments while ensuring that the difference between any point on $h(f_{ij})$ and its corresponding linear approximate value is no more than a given error η. We assume C is the minimum number of linear segments and $f_{ij}^0, f_{ij}^1, \cdots, f_{ij}^C$ are values on the X-axis for the end points of these segments. As variable f_{ij} is in the range of $[\frac{\lambda}{\mu}, B]$ from Constraints (14) and (17)) we have

$$f_{ij}^0 = \lceil\frac{\lambda}{\mu}\rceil, f_{ij}^C = B .$$

To find the minimum value of C, we start from the first point f_{ij}^0 to calculate the slope of the first segment, which ensures that the gap between this linear segment and the original curve is no more than η. Given this start point and the slope, we can obtain the end point of this segment that intersects with the original curve. This end point is also the start point of the second segment, denoted by f_{ij}^1. From there on, we repeat the above process until all segments are identified to cover the feasible range of f_{ij}. With the c-th linear segment and its slope denoted respectively by $G_c(f_{ij})$ and q_{ij}^c, we have

$$q_{ij}^c = \frac{h(f_{ij}^c) - h(f_{ij}^{c-1})}{f_{ij}^c - f_{ij}^{c-1}}, \tag{28}$$

$$G_c(f_{ij}) = q_{ij}^c \cdot (f_{ij} - f_{ij}^{c-1}) + h(f_{ij}^{c-1}). \tag{29}$$

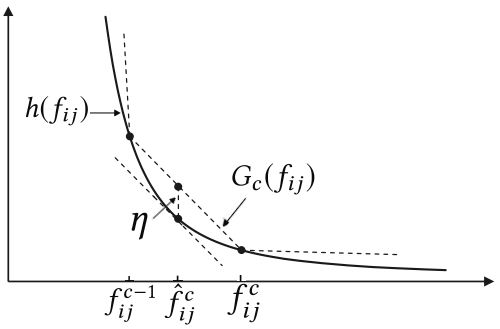

Fig. 4. The piece-wise approximation.

As shown in Figure 4, over the range of (f_{ij}^{c-1}, f_{ij}^c), there is a point where the gap is maximum, i.e., equal to η. With the X-coordinate of this point denoted by $\hat{f}_{ij}^c$ and based on the mathematical definition, we get the following equations:

$$\frac{\partial h(\hat{f}_{ij}^c)}{\partial f_{ij}} - q_{ij}^c = 0,\ G_c(\hat{f}_{ij}^c) - h(\hat{f}_{ij}^c) = \eta. \tag{30}$$

Specifically, if $h(f_{ij}^{c-1}) \le \eta$ for the start point of c-th segment, there is no feasible solution to Equation (30). In this case, we set the end point $f_{ij}^c = B$ while connecting the points of $(f_{ij}^{c-1}, h(f_{ij}^{c-1}))$ and $(B, h(B))$ to represent the last segment.

Therefore, given an error bound η, the values of $f_{ij}^1, \cdots, f_{ij}^C$ and slopes $q_{ij}^1, \cdots, q_{ij}^C$ can be calculated by Algorithm 1.

Algorithm 1 : Piece-wise Linearization

Initialization: $c = 1$ and $f_{ij}^{c-1} = \lceil\frac{\lambda}{\mu}\rceil$.
while $f_{ij}^{c-1} < B$ **and** $h(f_{ij}^{c-1}) > \eta$ **do**
  Calculating slope q_{ij}^c by solving the equation (30).
  With q_{ij}^c, calculate the f_{ij}^c based on (28).
  c=c+1.
end while
if $f_{ij}^{c-1} \ge B$ **then**
  $C = c - 1, f_{ij}^C = B$, and recalculate the q_{ij}^C based on (28).
else if $h(f_{ij}^{c-1}) \le \eta$ **then**
  $C = c, f_{ij}^C = B$, and calculate q_{ij}^C based on (28).
end if

Lemma 2. *The approximation error within each linear segment derived from Algorithm 1 is no more than η.*

The proof can be directly obtained from the above construction and is omitted here. With Algorithm 1, we approximate the non-linear term of $h(f_{ij})$ in the objective function via a set of linear segments with an error upper bounded by η. Let $G(f_{ij})$ denote the concatenated linear segments constructed by Algorithm 1. The objective function of $\min A^{ave}$ for OPT-O then can be replaced by the

following linear objective function and constraints:

$$\begin{aligned} \min\ & A_L^{ave} \\ \text{s.t. } & A_L^{ave} = \frac{|\mathcal{L}|}{\lambda} + \sum_{i\in\mathcal{N}}\sum_{j\in\mathcal{R}_i} G(f_{ij}); \quad (31) \\ & G(f_{ij}) \geq q_{ij}^c \cdot (f_{ij} - f_{ij}^{c-1}) + h(f_{ij}^{c-1}), \\ & (c = 1, 2, \cdots, C, f_{ij} \in [\frac{\lambda}{\mu}, B], i \in \mathcal{N}, j \in \mathcal{R}_i). \quad (32) \end{aligned}$$

The original OPT-O problem can be re-formulated into a new optimization problem, denoted by OPT-L.

$$\begin{aligned} \text{OPT-L}\quad & \min A_L^{ave} \\ & s.t.\ \text{Constraints: } (7), (8), (14), (17), (31), (32). \end{aligned}$$

In OPT-L, the liner segments concatenation $G(f_{ij})$ and the start point of each link f_{ij}^{c-1} have been calculated in the aforementioned steps. Here, we aim to solve the variables f_{ij} and $n_{ij}[b]$ for optimizing the linearized total time averaged AoI A_L^{ave}. The following theorem characterizes the gap between the optimal objective values of OPT-O and OPT-L.

Theorem 3. *The gap between the optimal objective values of OPT-O and OPT-L, ϵ, is upper bounded by*

$$\epsilon \leq \sum_{i\in\mathcal{N}}\sum_{j\in\mathcal{R}_i} \eta\ .$$

The proof of Theorem 3 is deferred to Appendix A.2.

With Algorithm 1 and Theorem 3, for any pre-setted approximation error ϵ, we can calculate the linear approximation error η and construct a series of linear segments to arrive at OPT-L. By solving OPT-L, we obtain the feasible solutions for OPT-O, with the approximation error to the optimal solution being no more than ϵ. OPT-L is in the form of mixed-integer linear programming, which is NP-hard in general. The commercial solvers (e.g., CPLEX) can be used to solve it directly, but they are not scalable to moderate or large-sized networks. Hence, this algorithm possesses the advantage of approaching the optimal solution as closely as we wish, but it is not scalable due to the concern of computation complexity.

4.2 Polynomial Time Algorithm

In this section, we design an efficient algorithm to solve OPT-O with polynomial time complexity while offering the guaranteed approximation gap to the optimal solution. The key challenge is to find the proper values of f_{ij} (i.e., link activation frequency) for all links toward minimizing AoI at all destination nodes. Hence, the essence of our algorithm design is to determine the link activation frequency of all links by taking interference avoidance into account.

Our algorithm includes two steps. In the first step, we construct an interference graph, in which each vertex represents a unique link in the network and each edge models the interference relationships between two links. The key idea here is to check Constraints (7) and (8), ensuring if two pairs of vertices (i.e., links) cannot be activated in the same channel due to the interference, half-duplex, or unicast constraints, the existence of an edge between these two vertex pairs.

In the second step, we iteratively determine the value for each vertex by assigning the channels to the respective link, which will be its activation frequency. Before illustrating the channels assignment strategy, we first discuss the lower bound of OPT-O, which will be used later in our algorithm design and its theoretical proof.

Lemma 3. *A lower bound for the objective of OPT-O, can be obtained by assigning each link with $B/3$ channels.*

Proof. Consider three consecutive links in a session, denoted as l_1, l_2, and l_3. l_1 will interfere with both l_2 and l_3 due to the half duplex and interference constraints, respectively, from Constraints (7) and (8). Similarly, l_2 will interfere with l_1 and l_3 while l_3 will interfere with l_1 and l_2. Hence, at least three consecutive links cannot be scheduled in the same channel. To derive the lower bound of OPT-O, we can reformulate it by only considering a series of three consecutive links. The reformulated problem is shown as follows

$$\begin{aligned} & \min A^{ave} = \frac{|\mathcal{L}|}{\lambda} + \sum_{i\in\mathcal{N}}\sum_{j\in\mathcal{R}_i} (\frac{1}{\mu f_{ij}} + \frac{\lambda^2}{(\mu f_{ij})^2(\mu f_{ij} - \lambda)}) \\ & s.t.\ f_{ij} + f_{jk} + f_{kh} \leq B, (i \in \mathcal{N}, j \in \mathcal{R}_i, k \in \mathcal{R}_j, h \in \mathcal{R}_k). \end{aligned}$$

This problem can be directly solved by employing the Lagrange multipliers method. The optimal solution results in all f_{ij} equal to $B/3$. Thus, a lower bound for OPT-O can be obtained by scheduling each link with $B/3$ channels. □

From Lemma 3, we can assign each link in the network with $B/3$ channels, then the lower bound of AoI, denoted by A_{LB}^{ave}, can be calculated as follows:

$$A_{LB}^{ave} = \frac{|\mathcal{L}|}{\lambda} + \sum_{i\in\mathcal{N}}\sum_{j\in\mathcal{R}_i} (\frac{1}{\mu B/3} + \frac{\lambda^2}{(\mu B/3)^2(\mu B/3 - \lambda)})\ . \quad (33)$$

Notably, such a lower bound is the minimal total time averaged AoI that the network can achieve without considering other constraints. The gap of averaged AoI between what is obtained by our algorithm and the optimal solution will be less than the difference between what is obtained by our algorithm and the lower bound.

Lemma 3 also implies that the averaged assignment of channels may help to minimize the AoI. This will guide the development of our channel allocation strategy in OPT-O. Algorithm 2 shows our design of determining the link activation frequency on each link. The main idea here is to assign the value to each vertex (i.e., assigning the number of channels to each link) and its neighboring vertices, based on the number of neighboring vertices, i.e., the degree of a vertex. We sort all vertices based on their degrees in the descending order and equally assign all channels to the vertex and its neighbors until all vertices are assigned with values. If one node has been assigned with a value in the previous step, this node will not be reassigned. After that, we continue to increment the value of each vertex by one each time in turn if there are more channels that can be added on, to further improve the AoI performance. This algorithm terminates when the values of all vertices cannot be further incremented.

Theorem 4. *The channel assignment solution derived from Algorithm 2 is feasible and our algorithm has the computation time*

Algorithm 2 : Channel Assignment

Input: $G = \{V, E\}$
for $v \in V$ **do**
  $v.value = 0$ and calculate the degree (i.e., the number of neighbor nodes) of v, recorded as $v.degree$.
end for
Sort V based on the descending order of $v.degree$.
for $v \in V$, selecting from the largest to lowest degrees **do**
  if $v.value = 0$ **then**
    $v.value = \lfloor B/(v.degree + 1) \rfloor$.
    Assign $v.value$ feasible channels to link v.
  end if
  for all v's neighbors v' **do**
    if $v'.value = 0$ **then**
      $v^{'}.value = v.value$.
      Assign $v^{'}.value$ feasible channels to link v'.
    end if
  end for
end for
while Links can be assigned with more channels **do**
  for $v \in V$ **do**
    if v can be assigned with more channels **then**
      Choose a channel b satisfying Constraints (7) and (8) while being occupied with the largest number of links, and assign it to v.
    end if
  end for
end while

complexity equal to $\mathcal{O}(D^2) + \mathcal{O}(DB)$, where D is the number of links and B is the number of channels.

Proof. In the interference graph, each vertex will interfere with all its neighbors. Thus, a vertex and all its neighbors can be considered as a mutual interference set. If we can assign channels to the vertices in each mutual interference set without interference, then our solution is feasible. In Algorithm 2, we start from the vertex with the largest degree and assign channels equally to it and its neighbors. Assume the largest degree is U_1. Then, this vertex and its neighbors will be assigned with $T_1 = B/(U_1 + 1)$ channels. In the second step, we select the vertex with the second largest degree, denote as U_2. For this vertex and neighboring vertices, if they are the neighbors of the first vertex, they have been assigned the channels of $T_1 = B/(U_1 + 1)$ and the channell allocation remains unchanged. For those that are not the neighbors of the first vertex, they will be assigned $T_2 = B/(U_2 + 1)$ channels. As $U_2 \leq U_1$, obviously, the total number of assigned channels among this second vertex and its neighbors will be no more than B as well. Thus, the channel assignment solution at this stage is still feasible. Similarly, in all the remaining steps, the channel assignment solution can be shown to be feasible. In the end, we add the channel to a link only if there exists any available channel that can be added on. Therefore, we can conclude the channel assignment solution from Algorithm 2 is feasible.

The computation complexity of this algorithm comes from four stages. First, calculating the degrees of links requires to search all link pairs, resulting in $\mathcal{O}(D^2)$ complexity, where D is the number of links. Second, sorting V based on the descending order of $v.degree$ requires $\mathcal{O}(D)$ complexity. Third, for each $v \in V$, assigning the values for it and all its neighbors resulting in $\mathcal{O}(D^2)$ complexity. In the end, if links can be assigned with more channels, we need to examine the pair of each link and each channel with the constraints, leading to the total of $\mathcal{O}(DB)$ complexity, where B is the number of channels. In total, our algorithm has the computation complexity of $\mathcal{O}(D^2) + \mathcal{O}(DB)$.

□

Next we will provide the theoretical performance bound for our algorithm.

Theorem 5. *Denote the minimum averaged AoIs from Algorithm 2 and OPT-O as A_*^{ave} and A_{opt}^{ave}, respectively, we have:*

$$A_*^{ave} \leq A_{opt}^{ave} + \frac{\mu B - 3\lambda - 3}{\mu B - 3\lambda} D \ , \tag{34}$$

where D is the number of links.

The proof of Theorem 5 is based on that the gap of averaged AoI between what is obtained by our algorithm A_*^{ave} and the optimal solution A_{opt}^{ave} will be less than the difference of upper bound and lower bound. The detailed proof can be found in Appendix A.3.

5 Evaluation

In this section, we provide the numerical results to illustrate AoI performance in OFDM-based multi-hop networks, where nodes are randomly placed in a 150 × 150 area. The source and destination nodes of each session are randomly selected among these nodes, with the shortest path being employed to find the route, although other routing methods may be used if needed. We randomly generate sessions in the network, with the total number of links ranging from 10 to 30. For generality, we normalize the units for distance, transmission range, interference range, packet generation rate, and a single channel's service rate with respect to appropriate values. The transmission range of each node is set to 40, while the interference range is specified in the respective performance studies. Given that there is no prior solution for AoI optimization in OFDM-based multi-hop wireless networks, we adopt two baseline channel scheduling policies for comparison, i.e., the Round Robin (RR) policy and the greedy policy. For the former, we assign links with channels in turn until no more link can be assigned without interference. For the latter, a link with less interference has a higher priority in getting assigned with more channels.

The goal of this section is twofold. First, we show AoI performance of our developed model and proposed algorithms by comparing their results with those of the RR policy to exhibit their advantage potentials in terms of minimizing AoI in OFDM-based multi-hop networks. Second, we illustrate the impact of different physical factors (i.e., channel amounts, the interference range, and the packet generation rate) on AoI.

This article has been accepted for publication in IEEE Transactions on Mobile Computing. This is the author's version which has not been fully edited and content may change prior to final publication. Citation information: DOI 10.1109/TMC.2022.3181038

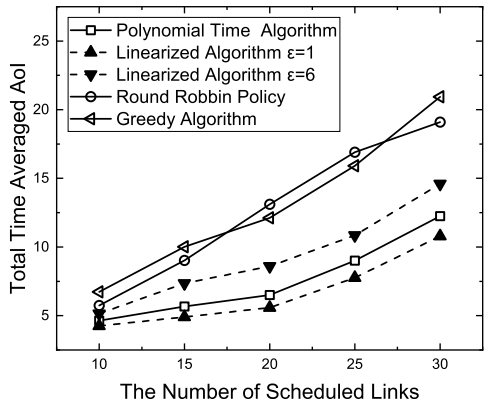

Fig. 5. The comparison of AoI among our solutions, RR policy, and greedy policy.

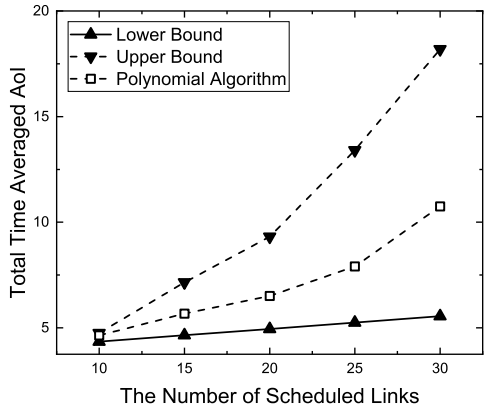

Fig. 6. AoI comparative results of our PTA, upper bound, and lower bound.

5.1 Comparisons

We set the interference range, the packet generation rate, and a single channel's service rate as 80, 0.80, and 1, respectively. In the linearized approximate solution, we set the gap values of $\epsilon = 1$ and $\epsilon = 6$, respectively. The number of sessions in the network grows when the link count rises from 10 to 30 and the number of channels is set to 50. Our experiment is conducted on an ASUS ROG GL702VS Laptop, equipped with Intel Core i7-7700HQ CPU clocking at 2.8 GHz. The laptop has 16 GB DRAM and runs Windows 10 Professional.

The AoI comparative results of our proposed solutions, the RR policy, and the greedy policy versus the scheduled link counts are shown in Figure 5. We observe that the AoI results obtained from both our proposed linearized algorithm (LA) and polynomial time algorithm (PTA) are always far better than those of the RR and greedy policies. Under the RR policy, links that cause high interference are assigned equally with other links, leading to low utilization of those channels assigned to high-interfering links. As a result, the total of link activation frequency is lower under the RR policy than under our proposed algorithms, rendering the RR policy to have higher AoI values. Under the greedy policy, the channel allocation among links is unbalanced since more interfered links are assigned with fewer channels. It results in AoI values close to those under the RR policy, having much higher AoI values than our proposed approaches.

When comparing LA and PTA, we can see, for $\epsilon = 1$, AoI is always better under LA than under PTA. However, when $\epsilon = 6$, LA underperforms PTA. This is expected as the large value of ϵ represents that LA's performance is far away from the optimal solution. In this case, its performance becomes worse than that of the PTA, signifying that our PTA solution is closer to the optimal solution. To make LA produce a near optimal solution, we can set the ϵ value as small as possible, but the computation complexity will increase accordingly.

We also plot the upper and the lower bounds of our PTA algorithm and compare them to our PTA performance results for a range of link amounts, as depicted in Figure 6. We observe when the number of links is small, PTA results are very close to the two bounds, demonstrating that our solution approaches the optimal one. Even with an increase in link amounts, the gap between two bounds increases, but our PTA is more close to the lower bound, at which the optimal solution resides. Thus, we can conclude that our PTA solution is close to the optimal one.

We then compare the running times of LA and PTA for various link counts and a range of available channels in the networks. Table 2 lists the running times of LA and PTA when varying the numbers of links and channels. From the last two columns, PTA is seen to be always much faster than LA. In particular, the running time of LA algorithm rises from 2.34 to 7234.67 seconds when the numbers of links and of channels increase respectively from 10 to 50 and 15 to 80 for $\epsilon = 1$. If the gap ϵ is set to a larger value, i.e., 30 and 50, the running times of LA drop but they are still much larger than those of the PTA. On the other hand, PTA always takes less than 1 second, clearly demonstrating its polynomial time advantages. Furthermore, when comparing the last three rows where the link numbers, channel amounts, and the interference range are all identical, the computation time of LA increases from $3761.74s$ to 7234.67 as ϵ drops from 50 to 1. The reason is that a smaller ϵ value results in more linear segments, which call for a much longer computation time.

In practice, the use of LA and PTA can be determined based on the network operator's demands and the network topology. If the network operator has a strict performance requirement while the network topology is simple, LA is a better choice, since it can approach the optimal solution as closely as desired. But if the performance demand is not strict and the network topology is complex, PTA is preferred, due to its fast computation.

5.2 Impacts of Physical Factors

We then explore the impact of such factors as channel amounts, interference range, and packet generation rate, on the resulting AoI. Here, we follow the similar setting as above and present the results of polynomial time algorithm only.

5.2.1 Impacts of Channel Amounts and Link Counts on AoI

The interference range is set to be 60. We first fix the bandwidth of each channel, by assuming the packet service rate to be 1. Figure 7 shows the AoI results when varying the

This article has been accepted for publication in IEEE Transactions on Mobile Computing. This is the author's version which has not been fully edited and content may change prior to final publication. Citation information: DOI 10.1109/TMC.2022.3181038

TABLE 2
Comparative running times between our linearized algorithm (LA) and polynomial time algorithm (PTA)

Links	Channels	ϵ	Interference Range	LA	PTA
10	15	1	60	2.34s	<1s
10	30	1	60	3.79s	<1s
20	30	1	60	20.68s	<1s
30	30	1	60	130.44s	<1s
30	50	1	60	727.12s	<1s
30	60	1	60	1576.59s	<1s
50	60	1	60	3611.81s	<1s
50	80	1	60	7234.67s	<1s
50	80	30	60	4031.91s	<1s
50	80	50	60	3761.74s	<1s

numbers of channels and links. In this figure, AoI values are seen to improve with an increase of the available channel amount. In particular, when the channel amount rises from 20 to 50, AoI decreases from 11.01 to 4.56, from 14.50 to 5.25, from 18.67 to 8.78, from 37.83 to 14.46, and from 50.46 to 20.20, respectively, under 10, 15, 20, 25, and 30 links. The reason is that more channels raise total bandwidth and can provide more activation opportunities for links, which can help lift the packet service rate on each link, thereby lowering destination nodes' AoI. On the other hand, an increase of the link amount degrades AoI performance. For example, when the link amount grows from 10, 15, 20, 25, to 30, the AoI value increases from 11.01 to 50.46, from 8.06 to 35.09, from 6.26 to 26.10, and from 4.56 to 20.20, respectively, corresponding to the networks with 20, 30, 40, and 50 channels. This is because, for given channel amounts, more links in the network will reduce each link's activation opportunity, leading to a lower packet service rate (i.e., link activation frequency) on each link and thus degrading AoI performance.

We next fix the total bandwidth to be 20 and assume the packet service rate of 1, corresponding to one unit bandwidth. Figure 8 shows the AoI results when varying the numbers of channels and links under fixed total bandwidth, in contrast to Figure 7 under fixed bandwidth per channel. The AoI values are still seen to improve with an increase in the channel amounts under different link counts. When the channel amount rises from 20 to 50, AoI decreases from 11.01 to 8.68, from 14.50 to 9.75, from 18.67 to 13.05, from 37.83 to 29.67, and from 50.46 to 38.21, respectively, under 10, 15, 20, 25, and 30 links. The reason is that, although the total bandwidth is fixed, more channels can offer much finer-grained scheduling among links, therefore helping to lower AoI values. However, due to the reduced packet service rate on each channel here (due to fixed total bandwidth), corresponding AoI values are larger when compared to those shown in Figure 7.

5.2.2 Impacts of Interference Range on AoI

We now explore the impact of interference range on AoI. We fix the number of channels to 40. Figure 9 depicts the AoI curves for varying interference ranges, with solid, dashed, and dotted lines corresponding respectively to the results of interference ranges of 60, 70, and 80. From this figure, AoI is observed to become worse with an increase in the interference range. The reason is that a wider interference range increases the interference density in the networks, thus reducing each link's activation opportunity, which in turn lowers the packet service rate on each link to hike AoI. Specifically, when the number of network links is only 10, small disparate AoI values result, due to the low interference density under all three interference ranges. But, when the number of network links increases to 30, interference becomes much denser under the interference range of 80 than under the interference range of 60. Thus, AoI performance in the former scenario degrades to a much larger value than the latter one.

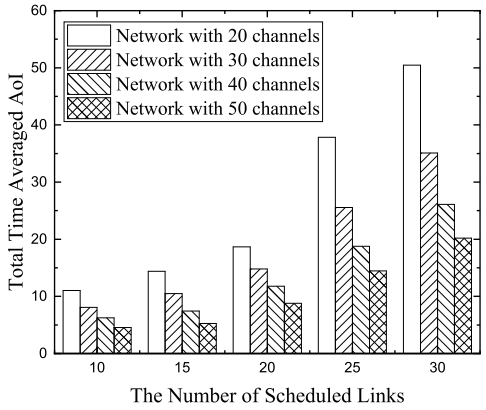

Fig. 7. The impact of channel amounts on AoI under different link counts with fixed bandwidth on each channel.

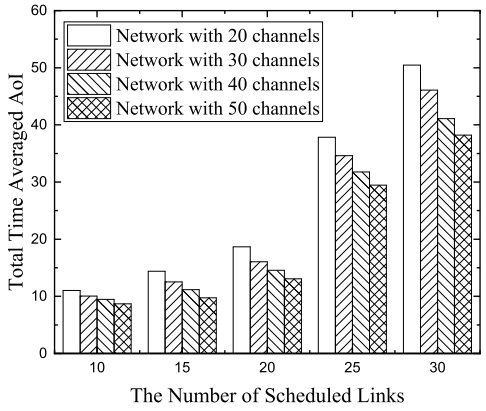

Fig. 8. The impact of channel amounts on AoI under different link counts with fixed total bandwidth.

5.2.3 Impacts of Packet Generation Rate on AoI

We now set the interference range as 60, the service rate on each channel as 1, and the number of sessions as 5 for 20 links in the network. Figure 10 shows AoI under 15 and 30 channels, with the packet generation rate varying from 0.1 to 0.9. From the curve of 15 channels, AoI is found to firstly decrease to the lowest point before moving up afterward. The reason lies in that when the packet generation rate is small, all generated packets are served immediately once arriving at a node, so AoI drops with faster packet delivery at destination nodes. After the packet generation rate rises above a threshold point, arrival packets cannot be served immediately at certain nodes, leading to some packets experiencing wait times there so that they are not delivered to

This article has been accepted for publication in IEEE Transactions on Mobile Computing. This is the author's version which has not been fully edited and content may change prior to final publication. Citation information: DOI 10.1109/TMC.2022.3181038

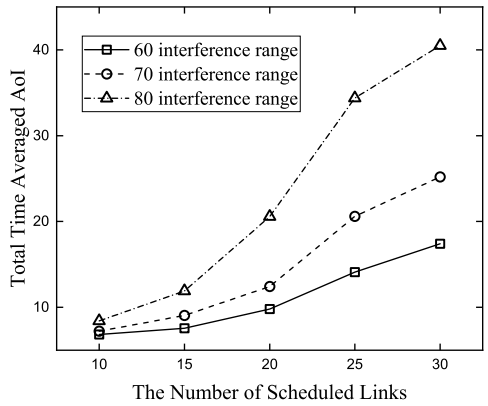

Fig. 9. The impact of interference ranges on AoI under different link counts.

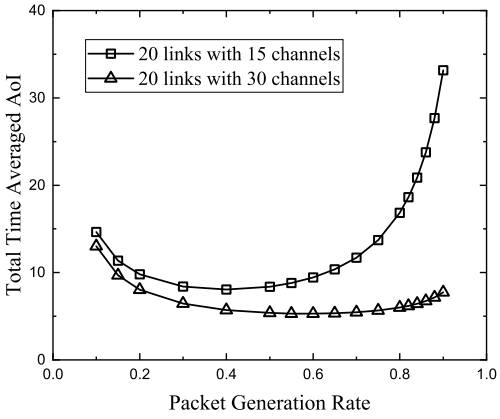

Fig. 10. The impact of packet generation rates on AoI under different channel counts.

destination nodes promptly. For the curve of 30 channels, we find that its lowest point is situated to the right side of that for 15 channels. This is expected as more channels increase the packet service rate and hence can handle higher packet generation rates. These results provide an insight into packet generation control for further AoI reduction.

6 Related Work

6.1 AoI in Single-hop Networks

AoI has been studied extensively in single-hop networks. Considerable previous work focuses on packet generation rate control, queue management, and the scheduling policy. In [1], the optimal generation rate with the *First Come First Served* (FCFS) scheduling policy has been derived to minimize AoI at destination nodes, with rate control also extended to the network with multiple sources [2]. It demonstrates that the optimal AoI is significantly different from the minimized delay. In [3], the zero-wait policy has been explored and found that it doesn't always minimize AoI. Meanwhile, various queuing packet management methods have been pursued in [4], [5], and [6], demonstrating that discarding old packets can help reduce time averaged AoI. Work in the scheduling policy has considered the *Last Generated First Served* (LGFS) queue discipline with/without preemption to analyze averaged AoI [7]. The optimized AoI under preemptive LGFS has been addressed for multi-server single-hop networks [8]. Replication in the LGFS policy has been considered recently [9], and it is shown to help improve AoI in a multi-server system, while an extended LGFS policy (i.e., Max-Age-First LGFS) has been addressed in [10]. All previous efforts deal with simple network settings, without taking into account the realistic network factors.

AoI has been pursued in the broadcast network [11], [12]. Specifically, [11] explores the long-run average AoI in the setting where a base station (BS) can receive packets from multiple sources and then broadcasts each packet to its destined user. In [12], the wireless broadcast network with unreliable channels is addressed for a BS to send information to multiple clients. The impact of channel access on AoI has started to receive attention. For example, in [17], the scheduled access with slotted ALOHA has been considered to schedule the packet transmission, while in [17], [18], the "take turns" channel access method is followed to schedule multiple terminals to communicate with one BS. In [19], the general TDMA modulation scheme was studied for AoI minimization and then [20] considered the multi-channel allocation for data transmission between one BS and different users.

The effort to consider AoI in different network environmental constraints has begun. For example, [13] and [14] have pursued energy replenishment and its impact on AoI. [15] has attempted to optimize AoI with throughput constraints, and [16] has studied AoI with general interference constraints, i.e., pre-determining the set of links that can be activated simultaneously. Besides, the IoT networks and network edges scenarios have also been studied to enlarge the scope from theoretical level to practical implementation. [32] considered the status sampling and updating behavior at the IoT network while accounting for an average energy cost constraint at the IoT device. In the large-scale IoT network with different time-triggered and event-triggered traffic, [33] proposed a spatiotemporal framework for optimizing the data freshness. For the network edges, the optimal sampling schedule is proposed to minimize AoI in [34]. In [35], authors condsidered a central station and a set of ground terminals via a mobile agent that can travel across the ground terminals, an AoI-based trajectory is then proposed to improve the data freshness. [36] studied the request and response behaviors to improve the actual freshness of data that only accounts for users' requests. Considering the industrial IoT, AoI optimization was studied to lift the average control system performance in [37], [38]. However, all these work limit the studied scope into the single-hop network and cannot be simply applied in the multi-hop setting, which differs from our work.

6.2 AoI in Multi-hop Networks

Prior studies on AoI in multi-hop networks limit their scopes to either a special network topology or an abstracted network setting. In [21], AoI is explored in the gossip network while [22] studies a two-hop network aiming at energy-harvesting. In [24], a two-hop network was studied to analyze AoI jointly with the packet coding problem, where sensors upload data to the edge server through the

sink node. [25] addressed the trade-off between the AoI and the average energy cost for a two-hop decode-and-forward (DF) relaying network. In [23], authors analyzed the AoI optimization in an IoT network with a two-hop relay. In [26], the LGFS with/without preemption at a source node is addressed for multi-hop networks where a source node transmits scheduled packets to different destination nodes. In [27], general interference constraints in multi-hop networks are considered in pursuit of AoI, but the considered models simplify the setting with pre-grouped interference-free sets and assume each set to have an activation probability. Our previous work [28] studied the AoI and throughput tradeoffs in the multi-hop network with flexible routing. However, the network setting is simplified with the deterministic packet generation behavior where the generation rate and time point are assumed to be constant.

Our work is sharply different from previous studies by (1) considering the general multi-hop network settings and (2) taking into account the realistic physical factors, such as channel access modulation (i.e., OFDM), wireless interference, and transmission routes.

7 Discussion

To the best of our knowledge, this work is the first one to advance the theoretical foundation of AoI in multi-hop wireless networks with a series of practical physical factors involved. Some limitations exist for this work as is presented, and they are to be addressed in our future work, as stated in sequence below.

First, the current work only focused on the AoI in OFDM channel access, while AoI in TDMA (or the hybrid of OFDM and TDMA)-based multi-hop networks remains open. From the spectrum utilization and throughput enhancement perspectives, OFDM and TDMA operate with no significant difference, where channels and time slots can play the same role to help activate network links. But from the optimizing information freshness perspective, they have fundamental differences in that all time slots represent a time sequence, where the activation of a link in different time slots has a substantial impact on the resulted AoI. With the discrete characteristic of time slots in a TDMA multi-hop network, its resulting AoI will be incremented with a slot-by-slot manner. Thus, the existing method to handle continuously increasing AoI cannot be applied here and the optimization problem is to exhibit as the integer problem, which is hard to be solved for the optimal results. Hence, a new method to represent the incremental of AoI with the consideration of TDMA characteristic has to be developed. Thus, it is more challenging to optimize AoI in TDMA-based multi-hop wireless networks, because, the ordering time slots to be activated among different links have to be taken into account as well, besides resource allocation. This requires to derive new AoI formula to capture the impact of such ordering relationships on AoI in TDMA.

Second, this work considered the multi-hop network setting where multiple sessions may intersect at some nodes but may not share the same link. This modeling assumption allows to better reveal the AoI performance variation influenced by plenty of practical issues existing in such a complex multi-hop network. The main concern comes from queuing and scheduling resulted from the multi-source problem at each shared link, since packets that arrive at the link from different sources may follow distinct distributions to behave irregularly. Hence, it is critical on how to schedule the transmission of packets from different sources. The new analysis of the queuing management and scheduling strategies in such a scenario is thus needed, exhibiting as an open and challenging problem.

Third, our simulation outcomes have revealed that the packet generation rate has a significant impact on AoI. Even such a problem has been well studied in single-hop networks, its pursuit in the multi-hop networks is yet to be explored. New challenges arise in the multi-hop setting if a tractable model is to be developed for capturing the relationships of the generation rate and AoI so as to obtain the optimal generation rate that yields the minimum AoI. Comparing to the single hop setting, new channel allocation strategies over different links, interference avoidance, queue modeling along each session, and AoI formula with the packet generation rate should be taken into account according to the characteristics of multi-hop networks, apparently a non-trivial endeavor, given that existing solutions for single-hop settings are inapplicable.

8 Conclusion

In this paper, we have addressed the AoI in multi-hop wireless networks for the first time by taking into account realistic network factors, including channel access modulations (i.e., OFDM) and wireless interference (i.e., unicast, half-duplex, and link interference avoidance). Specifically, we have developed a rigorous mathematical model to capture the impacts of channel allocations, link scheduling, wireless interference, and the queuing model on AoI, deriving a formula for AoI at destination nodes. Given AoI optimization based on our developed model is in the mixed integer non-linear form, the article provides two approximate algorithms to solve the problem. In the first algorithm, we employ the piece-wise linearization technique to transform the non-linear AoI formula into a set of linear constraints, enabling us to use the commercial solver to solve it. This algorithm approaches closely to the optimal solution by properly setting a small error bound, but it does not scale. In the second algorithm, a polynomial time solution is proposed to obtain results fast while confining the gap between its solution and the optimal one. Numerical AoI performance results under our developed approximation solutions have been obtained for OFDM-based wireless networks. The results confirm that our developed solutions exhibit far better AoI performance than their Round Robin policy counterpart.

Acknowledgment

This work was supported in part by NSF under Grants 1763620, 1948374, and 2019511. Dr. Qin's work was supported in part by CIC Young Elite Scientists Sponsorship Program under Grant No. 2021QNRC001. Any opinion and findings expressed in the paper are those of the authors and do not necessarily reflect the view of funding agency.

REFERENCES

[1] S. Kaul, R. Yates, and M. Gruteser, "Real-time status: How often should one update?" in *Proceedings of IEEE International Conference on Computer Communications (INFOCOM)*, 2012, pp. 2731–2735.

[2] R. D. Yates and S. Kaul, "Real-time status updating: Multiple sources," in *Proceedings of IEEE International Symposium on Information Theory (ISIT)*, 2012, pp. 2666–2670.

[3] Y. Sun, E. Uysal-Biyikoglu, R. Yates, C. E. Koksal, and N. B. Shroff, "Update or wait: How to keep your data fresh," in *Proceedings of IEEE International Conference on Computer Communications (INFOCOM)*, 2016, pp. 1–9.

[4] M. Costa, M. Codreanu, and A. Ephremides, "Age of information with packet management," in *Proceedings of IEEE International Symposium on Information Theory (ISIT)*, 2014, pp. 1583–1587.

[5] ——, "On the age of information in status update systems with packet management," *IEEE Transactions on Information Theory*, vol. 62, no. 4, pp. 1897–1910, 2016.

[6] N. Pappas, J. Gunnarsson, L. Kratz, M. Kountouris, and V. Angelakis, "Age of information of multiple sources with queue management," in *Proceedings of IEEE International Conference on Communications (ICC)*, 2015, pp. 5935–5940.

[7] S. K. Kaul, R. D. Yates, and M. Gruteser, "Status updates through queues," in *Proceedings of Annual Conference on Information Sciences and Systems (CISS)*, 2012, pp. 1–6.

[8] A. M. Bedewy, Y. Sun, and N. B. Shroff, "Optimizing data freshness, throughput, and delay in multi-server information-update systems," in *Proceedings of IEEE International Symposium on Information Theory (ISIT)*, 2016, pp. 2569–2573.

[9] ——, "Minimizing the age of information through queues," *IEEE Transactions on Information Theory*, vol. 65, no. 8, pp. 5215–5232, 2019.

[10] Y. Sun, E. Uysal-Biyikoglu, and S. Kompella, "Age-optimal updates of multiple information flows," in *Proceedings of IEEE Conference on Computer Communications Workshops (INFOCOM)*. IEEE, 2018, pp. 136–141.

[11] Y.-P. Hsu, E. Modiano, and L. Duan, "Scheduling algorithms for minimizing age of information in wireless broadcast networks with random arrivals," *IEEE Transactions on Mobile Computing*, vol. 19, no. 12, pp. 2903–2915, 2019.

[12] I. Kadota, A. Sinha, E. Uysal-Biyikoglu, R. Singh, and E. Modiano, "Scheduling policies for minimizing age of information in broadcast wireless networks," *Transactions on Networking*, vol. 26, no. 6, pp. 2637–2650, 2018.

[13] B. T. Bacinoglu, E. T. Ceran, and E. Uysal-Biyikoglu, "Age of information under energy replenishment constraints," in *Proceedings of Information Theory and Applications Workshop (ITA)*, 2015, pp. 25–31.

[14] R. D. Yates, "Lazy is timely: Status updates by an energy harvesting source," in *Proceedings of IEEE International Symposium on Information Theory (ISIT)*, 2015, pp. 3008–3012.

[15] I. Kadota, A. Sinha, and E. Modiano, "Optimizing age of information in wireless networks with throughput constraints," in *Proceedings of IEEE International Conference on Computer Communications (INFOCOM)*, 2018, pp. 1844–1852.

[16] R. Talak, S. Karaman, and E. Modiano, "Optimizing information freshness in wireless networks under general interference constraints," in *Proceedings of ACM International Symposium on Mobile Ad Hoc Networking and Computing (MobiHoc)*, 2018, pp. 61–70.

[17] R. D. Yates and S. K. Kaul, "Status updates over unreliable multiaccess channels," in *Proceedings of IEEE International Symposium on Information Theory (ISIT)*, 2017, pp. 331–335.

[18] Z. Jiang, B. Krishnamachari, X. Zheng, S. Zhou, and Z. Niu, "Decentralized status update for age-of-information optimization in wireless multiaccess channels," in *Proceedings of IEEE International Symposium on Information Theory (ISIT)*, 2018, pp. 2276–2280.

[19] T.-W. Kuo, "Minimum age TDMA scheduling," in *Proceedings of IEEE International Conference on Computer Communications (INFOCOM)*, 2019, pp. 2296–2304.

[20] Z. Qian, F. Wu, J. Pan, K. Srinivasan, and N. B. Shroff, "Minimizing age of information in multi-channel time-sensitive information update systems," in *Proceedings of IEEE International Conference on Computer Communications (INFOCOM)*, 2020, pp. 446–455.

[21] J. Selen, Y. Nazarathy, L. L. H. Andrew, and L. V. Hai, "The age of information in gossip networks," *Environmental Technology*, vol. 27, no. 8, pp. 863–873, 2013.

[22] A. Arafa and S. Ulukus, "Age-minimal transmission in energy harvesting two-hop networks," in *Proceedings of IEEE Global Communications Conference (GLOBECOM)*, 2017, pp. 1–6.

[23] J. Lou, X. Yuan, and N.-F. Tzeng, "Instant AoI optimization in IoT networks with packet combination," in *Proceedings of IEEE International Conference on Sensing, Communication and Networking (SECON)*, 2020, pp. 1–9.

[24] T.-T. Chan, H. Pan, and J. Liang, "Age of information with joint packet coding in industrial iot," *IEEE Wireless Communications Letters*, vol. 10, no. 11, pp. 2499–2503, 2021.

[25] M. Xie, J. Gong, and X. Ma, "Age and energy tradeoff for short packet based two-hop decode-and-forward relaying networks," in *Proceedings of IEEE Wireless Communications and Networking Conference (WCNC)*, 2021, pp. 1–6.

[26] A. M. Bedewy, Y. Sun, and N. B. Shroff, "The age of information in multihop networks," *Transactions on Networking*, vol. 27, no. 3, pp. 1248–1257, 2019.

[27] R. Talak, S. Karaman, and E. Modiano, "Minimizing age-of-information in multi-hop wireless networks," in *Proceedings of Allerton Conference on Communication, Control, and Computing (Allerton)*, 2017, pp. 486–493.

[28] J. Lou, X. Yuan, S. Kompella, and N.-F. Tzeng, "AoI and throughput tradeoffs in routing-aware multi-hop wireless networks," in *Proceedings of IEEE International Conference on Computer Communications (INFOCOM)*, 2020, pp. 476–485.

[29] C. Perkins, E. Belding, and S. R. Das, "Ad-hoc on-demand distance vector routing," RFC 3561, Tech. Rep., 2003.

[30] D. Johnson, Y.-c. Hu, and D. Maltz, "The dynamic source routing protocol (DSR) for mobile ad hoc networks for IPv4," RFC 4728, Tech. Rep., 2007.

[31] P. J. Burke, "The output of a queuing system," *Operations Research*, vol. 4, no. 6, pp. 699–704, 1956.

[32] B. Zhou and W. Saad, "Optimal sampling and updating for minimizing age of information in the internet of things," in *Proceedings of IEEE Global Communications Conference (GLOBECOM)*, 2018, pp. 1–6.

[33] M. Emara, H. Elsawy, and G. Bauch, "A spatiotemporal model for peak AoI in uplink IoT networks: Time versus event-triggered traffic," *IEEE Internet of Things Journal*, vol. 7, no. 8, pp. 6762–6777, 2020.

[34] C. Li, S. Li, and Y. T. Hou, "A general model for minimizing age of information at network edge," in *Proceedings of IEEE International Conference on Computer Communications (INFOCOM)*, 2019, pp. 118–126.

[35] V. Tripathi, R. Talak, and E. Modiano, "Age optimal information gathering and dissemination on graphs," in *Proceedings of IEEE International Conference on Computer Communications (INFOCOM)*, 2019, pp. 2422–2430.

[36] B. Yin, S. Zhang, Y. Cheng, L. X. Cai, Z. Jiang, S. Zhou, and Z. Niu, "Only those requested count: Proactive scheduling policies for minimizing effective age-of-information," in *Proceedings of IEEE International Conference on Computer Communications (INFOCOM)*, 2019, pp. 109–117.

[37] X. Wang, C. Chen, J. He, S. Zhu, and X. Guan, "AoI-aware control and communication co-design for industrial IoT systems," *IEEE Internet of Things Journal*, pp. 1–1, 2020.

[38] M. Li, C. Chen, C. Hua, and X. Guan, "Learning-based autonomous scheduling for AoI-aware industrial wireless networks," *IEEE Internet of Things Journal*, vol. 7, no. 9, pp. 9175–9188, 2020.

Jiadong Lou (S'20) received the B.S. degree from School of Computer Science and Technology, Harbin Institute of Technology, in 2018. He is currently working toward the Ph.D. degree at the School of Computing and Informatics, University of Louisiana at Lafayette, Lafayette, LA, USA. His research interests include networking, mobile applications analysis, network protocols security, and security and privacy.

This article has been accepted for publication in IEEE Transactions on Mobile Computing. This is the author's version which has not been fully edited and content may change prior to final publication. Citation information: DOI 10.1109/TMC.2022.3181038

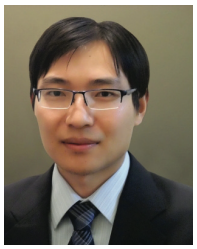

Xu Yuan (M'16-SM'22) received the B.S. degree from the College of Information Technology, Nankai University, Tianjin, China, in 2009, and the Ph.D. degree from the Bradley Department of Electrical and Computer Engineering, Virginia Tech, Blacksburg, VA, USA, in 2016. From 2016 to 2017, he was a Post-Doctoral Fellow of Electrical and Computer Engineering with the University of Toronto, Toronto, ON, Canada. He is currently a Hardy Edmiston Endowed Assistant Professor in the School of Computing and Informatics at the University of Louisiana at Lafayette, Lafayette, LA, USA. He was the receipt of NSF CRII Award and NSF CAREER Award. His research interest focuses on artificial intelligence, cybersecurity, networking and cyber-physical system.

Purushottam Sigdel (S'16–M'20) received the BE degree in electronics and communication engineering, in 2000, and the MS degree and the Ph.D. degree from Center for Advanced Computer Studies, the University of Louisiana at Lafayette, in 2014 and 2020, respectively. From 2020 to 2021, he was a Visiting Assistant Professor in School of Computing and Informatics at the University of Louisiana at Lafayette. He is currently a Research Engineer at K&A Engineering Consulting, NY, USA. His research interests include data compression, distributed computing, storage systems, and systems architecture.

Xiaoqi Qin (S'13–M'16) received her B.S., M.S., and Ph.D. degrees from Electrical and Computer Engineering with Virginia Tech. She is currently an Associate Professor in School of Information and Communication Engineering with Beijing University of Posts and Telecommunication (BUPT). Her research focuses on exploring performance limits of next-generation wireless networks, and developing innovative solutions for intelligent and concise machine-type communications.

Sastry Kompella (S'04-M'07-SM'12) received his Ph.D. degree in computer engineering from Virginia Tech, Blacksburg, Virginia, in 2006. He is currently the Section Head of the U.S. Naval Research Laboratory, Wireless Network Research Section under the Information Technology Division, Washington, DC, USA. His research interests include various aspects of wireless networks, from mobile ad hoc to underwater acoustic networks, with the specific focus towards cognitive and cooperative network optimization, programmable networking and fundamental limits of information latency.

Nian-Feng Tzeng (M'86-SM'92-F'10-LF'22) has been with Center for Advanced Computer Studies, School of Computing and Informatics, the University of Louisiana at Lafayette, since 1987. His current research interest include the areas of high-performance computer systems, and parallel and distributed processing. He was on the editorial board of the IEEE Transactions on Parallel and Distributed Systems, 1998 – 2001, and on the editorial board of the IEEE Transactions on Computers, 1994 – 1998. He was the chair of Technical Committee on Distributed Processing, the IEEE Computer Society, from 1999 till 2002. He is the recipient of the Outstanding Paper Award of the 10th IEEE International Conference on Distributed Computing Systems, May 1990, and received the University Foundation Distinguished Professor Award, in 1997.

APPENDIX

A.1 Proof of Theorem 2

Proof. According to the relationship of time averaged AoIs between two consecutive nodes in Theorem 1, we can derive the averaged AoI at destination node d_l by recursive derivation from source node s_l's successor (denoted as a) on path P_l:

$$A^l_{d_l} = A^l_a + \lambda \sum_{i\in\mathcal{P}_l, i\neq s_l, d_l} E[I^l_{s_l} M^l_{ij}] \,. \tag{35}$$

Based on Lemma 1, we have shown that the transmission process at each node can be modeled as an FCFS $M/M/1$ queuing process. As the transmission from source node s_l to its successor a is a one-hop transmission, the time averaged AoI derived in [1] for single-hop systems with the FCFS $M/M/1$ queuing model can be directly applied here. That is, the time averaged AoI at node a equals:

$$A^l_a = \lambda\big(E[I^l_{s_l} M^l_{s_l a}] + \frac{E[I^l_{s_l}]^2}{2}\big). \tag{36}$$

From [1], the average product of the generation interval time and the system time in an FCFS M/M/1 queuing system can be calculated as:

$$E[I^l_{s_l} M^l_{ij}] = \frac{\lambda}{\mu^2_{ij}(\mu_{ij}-\lambda)} + \frac{1}{\lambda\mu_{ij}}, \tag{37}$$

With (36), (37), and (17), we have the time averaged AoI at destination node d_l (i.e., (35)) as given by:

$$\begin{aligned}
A^l_{d_l} =& A^l_a + \lambda \sum_{i\in\mathcal{P}_l, i\neq s_l, d_l} E[I^l_{s_l} M^l_{ij}] \\
=& \lambda\big(E[I^l_{s_l} M^l_{s_l a}] + \frac{E[{I^l_{s_l}}^2]}{2}\big) + \lambda \sum_{i\in\mathcal{P}_l, i\neq s_l, d_l} E[I^l_{s_l} M^l_{ij}] \\
=& \lambda\frac{E[{I^l_{s_l}}^2]}{2} + \lambda \sum_{i\in\mathcal{P}_l, i\neq d_l} E[I^l_{s_l} M^l_{ij}] \\
=& \frac{1}{\lambda} + \sum_{i\in\mathcal{P}_l, i\neq d_l} \big[\frac{1}{\mu_{ij}} + \frac{\lambda^2}{\mu^2_{ij}(\mu_{ij}-\lambda)}\big] \\
=& \frac{1}{\lambda} + \sum_{i\in\mathcal{P}_l, i\neq d_l} \big(\frac{1}{\mu f_{ij}} + \frac{\lambda^2}{(\mu f_{ij})^2(\mu f_{ij}-\lambda)}\big),
\end{aligned} \tag{38}$$

where $E[{I^l_{s_l}}^2] = 2/\lambda^2$ since the generation process is an exponential distribution with rate λ. □

A.2 Proof of Theorem 3

Proof. Suppose the optimal solution of OPT-O is $\varphi^*_{OPT-O} = \{n^*_{ij}[b], f^*_{ij}\}$ with the objective value being A^{ave*}_O. As the solution φ^*_{OPT-O} meets all constraints in OPT-L, we can construct a feasible solution (denoted as φ_{OPT-L}) with its n and f values identical to those in φ^*_{OPT-O}, and $G(f_{ij})$ is solved via those values. Denoting the objective value of the solution φ_{OPT-L} as A^{ave}_L, we have:

$$\begin{aligned} A^{ave}_L - A^{ave*}_O &= \frac{|\mathcal{L}|}{\lambda} + \sum_{i\in\mathcal{N}}\sum_{j\in\mathcal{R}_i} G(f_{ij}) - \frac{|\mathcal{L}|}{\lambda} - \sum_{i\in\mathcal{N}}\sum_{j\in\mathcal{R}_i} h(f^*_{ij}) \\ &= \sum_{i\in\mathcal{N}}\sum_{j\in\mathcal{R}_i} \big(G(f_{ij}) - h(f^*_{ij})\big) \le \sum_{i\in\mathcal{N}}\sum_{j\in\mathcal{R}_i} \eta\,, \end{aligned}$$

where the last inequality is derived from Lemma 2. We let $\epsilon = \sum_{i\in\mathcal{N}}\sum_{j\in\mathcal{R}_i}\eta$ and denote φ^*_{OPT-L} as the optimal solution for OPT-L, with the objective value of A^{ave*}_L. As A^{ave}_L is the objective value of a feasible solution, we have $A^{ave*}_L \le A^{ave}_L$. As a result, $A^{ave*}_L - A^{ave*}_O \le A^{ave}_L - A^{ave*}_O \le \epsilon$. □

A.3 Proof of Theorem 5

Proof. Denote $\bar{N}$ as the largest degree among all vertices. According to Algorithm 2, the value of each vertex (i.e., channels assigned to the respective link) should be no less than $\lfloor B/(\bar{N}+1)\rfloor$. That is, the minimum link activation frequency $f_{min} \doteq \lfloor B/(\bar{N}+1)\rfloor$ is a feasible solution to OPT-O. Denote the achievable AoI with f_{min} as A^{ave}_{UB}, we have:

$$A^{ave}_{UB} = \frac{|\mathcal{L}|}{\lambda} + \sum_{i\in\mathcal{N}}\sum_{j\in\mathcal{R}_i} \Big(\frac{1}{\mu f_{min}} + \frac{\lambda^2}{(\mu f_{min})^2(\mu f_{min}-\lambda)}\Big)\,.$$

From Eqn. (33), we already have the lower bound A^{ave}_{LB}. Thus, the gap of averaged AoI between our algorithm A^{ave}_* and the optimal solution A^{ave}_{opt} will be less than the difference of upper bound A^{ave}_{UB} and lower bound A^{ave}_{LB}. We have:

$$\begin{aligned} A^{ave}_* - A^{ave}_{opt} &\le A^{ave}_{UB} - A^{ave}_{LB} \\ &= \frac{|\mathcal{L}|}{\lambda} + \sum_{i\in\mathcal{N}}\sum_{j\in\mathcal{R}_i} \Big(\frac{1}{\mu f_{min}} + \frac{\lambda^2}{(\mu f_{min})^2(\mu f_{min}-\lambda)}\Big) \\ &\quad - \Big(\frac{|\mathcal{L}|}{\lambda} + \sum_{i\in\mathcal{N}}\sum_{j\in\mathcal{R}_i} \Big(\frac{1}{\mu B/3} + \frac{\lambda^2}{(\mu B/3)^2(\mu B/3-\lambda)}\Big)\Big) \\ &\le \sum_{i\in\mathcal{N}}\sum_{j\in\mathcal{R}_i} \Big(\frac{1}{\mu\lfloor B/(\bar{N}+1)\rfloor - \lambda} - \frac{1}{\mu B/3-\lambda}\Big)\,. \end{aligned} \tag{39}$$

Based on (17), we have $\lfloor \mu B/(\bar{N}+1)\rfloor > \lambda/\mu$, then

$$\begin{aligned} A^{ave}_* - A^{ave}_{opt} &\le \sum_{i\in\mathcal{N}}\sum_{j\in\mathcal{R}_i} \Big(\frac{1}{\mu\lfloor B/(\bar{N}+1)\rfloor - \lambda} - \frac{1}{\mu B/3-\lambda}\Big) \\ &\le \sum_{i\in\mathcal{N}}\sum_{j\in\mathcal{R}_i} \Big(\frac{1}{\mu(\lfloor \lambda/\mu\rfloor + 1) - \lambda} - \frac{1}{\mu B/3-\lambda}\Big) \\ &= \frac{\mu B - 3\lambda - 3}{\mu B - 3\lambda} D, \end{aligned} \tag{40}$$

where D is the number of links in the network. As a result, we have the gap of our algorithm to the optimal objective value being no more than $\frac{\mu B-3\lambda-3}{\mu B-3\lambda} D$. □